# Photon Correlation Spectroscopy

H. J. Carmichael,[1] P. Kochan,[1] and B. C. Sanders[2]
[1]*Department of Physics, University of Oregon, Eugene, Oregon 97403*
[2]*School of Mathematics, Physics, Computing and Electronics, Macquarie University, NSW 2109, Australia*
(Received 11 January 1996)

A spectroscopic technique for observing excited state resonances in nonperturbative cavity QED is proposed. The feasibility of experiments is demonstrated by a quantum trajectory simulation. [S0031-9007(96)00715-6]

PACS numbers: 42.50.Ct, 42.50.Ar

A two-state atom interacting with a resonant mode of the radiation field is the elementary system underlying the Planck hypothesis and the Einstein theory of spontaneous and stimulated emission. In its modern conception the physics of this system is more subtle, however, than either Planck or Einstein anticipated. According to quantum mechanics, the interaction produces eigenstates which entangle the atom with the field. For excitation by $n \geq 1$ quanta there are two such states with energies $E_{n,\pm} = E_0 + \hbar(n\omega_0 \pm \sqrt{n}\, g)$, where $E_0$ is the energy of the ground state, $\omega_0$ is the resonance frequency, and $g$ is the dipole coupling constant. While these eigenstates and eigenenergies have been known for three decades, and have been featured in numerous theoretical publications, as Jaynes and Cummings recognized in their seminal work on the problem, observable consequences of the atom-field entanglement are extremely difficult to detect [1]. In particular, a direct spectroscopic observation of the entangled-state resonances is only now becoming a reasonable proposition.

Observations of the ground of first excited state doublet were first reported for atomic systems [2–5], and recently also for semiconductor heterostructures [6–8]. This doublet is a robust feature common to many systems, however. It arises from normal modes wherever two coupled harmonic oscillators model the linear interaction between the radiation field and matter. Most importantly, it is predicted by a semiclassical calculation (no atom-field entanglement) without diagonalizing any quantum Hamiltonian. The above spectrum is characterized by the $\sqrt{n}$, the signature of its excited states. None of the quoted experiments involve systems which possess this excited state spectrum.

The system of one atom interacting with one mode of the radiation field has been realized using Rydberg atoms and superconducting microwave cavities. Here the Rabi nutation in a few-photon field contains information on the excited state spectrum, and while early experiments measured time series that are too short to allow splitting frequencies to be determined [9], a recent experiment with circular Rydberg states is able to determine these frequencies [10]. In this Letter we are concerned with the optical frequency regime. At optical frequencies few-photon nonperturbative interactions are possible in high finesse Fabry-Pérot cavities [4], and standard nonlinear spectroscopy might be used to detect two-quanta or three-quanta entangled-state resonances. Such measurements face a unique set of difficulties, however. In a standing-wave $\mathrm{TEM}_{00}$ mode, the dipole coupling constant varies with the position of the atom as

$$g(r,\theta) = g_{\max}\cos\theta e^{-r^2/w_0^2}, \qquad \theta = 2\pi z/\lambda, \tag{1}$$

where $z$ locates the atom along the cavity axis, $r = (x^2 + y^2)^{1/2}$ is the distance of the atom from the cavity axis, and $w_0$ is the mode waist. Because of the small wavelength (and short photon lifetime) eliminating this variation is very difficult in an optical cavity. We analyze the consequences of the spatial variation of $g$ for atoms produced in an atomic beam and propose a spectroscopic technique to overcome the difficulties it creates. We demonstrate the feasibility of experiments with a quantum trajectory simulation.

The atomic beam travels in the $x$ direction and intersects the cavity axis at $z = 0$. The beam extends a distance $M\lambda/2$ along the cavity axis ($M$ an integer) and to infinity in the plane perpendicular to the axis. In this configuration, not only $g$, but even the number of interacting atoms is undefined, since the interaction volume is not bounded. Our first task, therefore, is to define the conditions which correspond to one atom interactions. To this end it is convenient to introduce the finite volume $V$ comprised of the $M$ disconnected regions—each centered on an antinode—enclosed by the surface $g(r,\theta)/g_{\max} = F < 1$; thus, $0 \leq |\theta| \leq \cos^{-1} F$, $0 \leq r^2/w_0^2 \leq \ln(\cos\theta/F)$, and

$$V = M\lambda w_0^2 I(F), \qquad I(F) = \int_F^1 dx\, \frac{\cos^{-1} x}{x}. \tag{2}$$

Clearly $V \to \infty$ as $F \to 0$.

In this system a ground to first excited state doublet appears for atomic beam densities above a minimum set by the atomic and cavity linewidths [2–4]. The splitting frequency is determined by the effective (collective) dipole coupling constant

$$g_{\mathrm{eff}} = \sqrt{N_{\mathrm{eff}}}\, g_{\max}, \qquad N_{\mathrm{eff}} = \sum_{j=1}^{N} \cos^2\theta_j e^{-2r_j^2/w_0^2}, \tag{3}$$

  

where $N$ is the number of atoms in $V$. $g_{\rm eff}$ is a stochastic variable due to the time dependence of the atomic positions—$x_j(t) = v_j(t - t_j)$, $y_j(t) = y_j^0$, $\theta_j(t) = \theta_t^0$, where $v_j$, $t_j$, $y_j^0$, and $\theta_j^0$ are all random variables. Of course, with $F \neq 0$, $N$ also fluctuates in time, but these fluctuations become negligible as $F \to 0$. For atoms created independently and randomly, at constant rate, in each velocity class, $N$ obeys a Poisson distribution and the atoms are uniformly distributed in space. We therefore expand the probability density for $g_{\rm eff}$ in the form

$$P(g_{\rm eff}) = \sum_N \frac{\overline{N}^N}{N!}\, e^{-\overline{N}} P(g_{\rm eff}\,|\,N)\,, \tag{4}$$

where $\overline{N}$ is the mean of $N$ and $P(g_{\rm eff}\,|\,N)$ is a conditional probability density—in particular, for one atom, uniformly distributed in $V$, Eq. (1) gives

$$P(g_{\rm eff}\,|\,1) = I(F)^{-1}\,\frac{\cos^{-1}(g_{\rm eff}/g_{\rm max})}{g_{\rm eff}}\,, \tag{5}$$

$1 \geq g_{\rm eff}/g_{\rm max} \geq F$. The mean of $N_{\rm eff}$ is

$$\overline{N}_{\rm eff} = \frac{1}{4}\,\overline{N} I(F)^{-1}[F\sqrt{1 - F^2} + (1 - 2F^2)\cos^{-1}F]\,, \tag{6}$$

with $\lim_{F\to 0} \overline{N}_{\rm eff} \to \overline{N}^0_{\rm eff} \equiv \rho_A M \lambda \pi w_0^2/8$, where $\rho_A$ is the atomic beam density. $\overline{N}^0_{\rm eff}$ is the average number of atoms in the cylinder $r < w_0/2$; we quote it, following [4], as a measure of $\rho_A$.

Clearly one atom interactions dominate at low atomic beam densities. What, however, defines low densities in a quantitative way? Mathematically, a limit at constant volume is the easiest to take. Here, with $F \ll 1$ constant, $\overline{N}^0_{\rm eff} \to 0$ as $\overline{N} \to 0$, and for $\overline{N} \ll 1$ we may approximate $P(g_{\rm eff})$ by $(1 - \overline{N})\delta(g_{\rm eff}) + \overline{N} P(g_{\rm eff}\,|\,1)$. But the condition $\overline{N} \ll 1$ depends on $F$, and is certainly too restrictive when $F$ is very small. The more meaningful limit is taken at constant density: $\overline{N} \to \infty$, $F \to 0$, with $\overline{N}^0_{\rm eff} \ll 1$ constant. This limit is difficult to evaluate exactly, but if $g_{\rm eff}$ is not too small an approximation may be made. Note that at low densities the probability to find two or more atoms within a given distance of the cavity axis is small; significant values of $g_{\rm eff}$ are realized when one, and only one, atom comes close to the axis. We therefore set $P(g_{\rm eff}\,|\,N) \approx N P(g_{\rm eff}\,|\,1)$ to obtain

$$P(g_{\rm eff}) \to \lim_{F\to 0} \overline{N} P(g_{\rm eff}\,|\,1) = \overline{N}^0_{\rm eff}\,\frac{8}{\pi}\,\frac{\cos^{-1}(g_{\rm eff}/g_{\rm max})}{g_{\rm eff}}\,. \tag{7}$$

This expression is correct to lowest order in $\overline{N}^0_{\rm eff}$ for $g_{\rm eff}/g_{\rm max} \gg \overline{N}^0_{\rm eff}$. The main error in the approximation is that Eq. (7) is more singular at the origin than the exact distribution, which is, of course, normalizable while Eq. (7) is not. The approximate expression is sufficient for our purposes. It shows that one-atom interactions dominate when $\overline{N}^0_{\rm eff} \ll 1$; at such densities the tail of $P(g_{\rm eff})$ is proportional to the conditional distribution $P(g_{\rm eff}\,|\,1)$.

To illustrate these ideas Fig. 1 compares results for $P(g_{\rm eff})$ obtained from Monte Carlo simulations

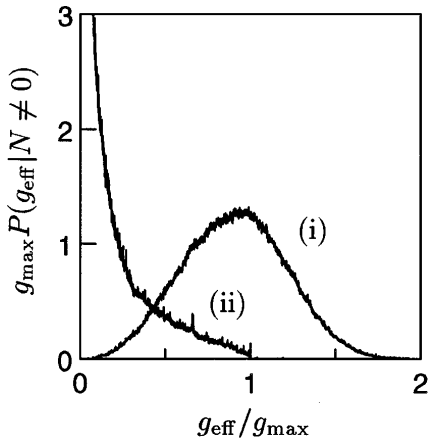


FIG. 1. Distribution of $g_{\rm eff}$: (i) $\overline{N}^0_{\rm eff} = 1$, $F = 0.1$; (ii) $\overline{N}^0_{\rm eff} = 0.02$, $F = 0.01$.

with $\overline{N}^0_{\rm eff} = 1$ and $\overline{N}^0_{\rm eff} = 0.02$. We have subtracted $e^{-\overline{N}}\delta(g_{\rm eff})$ from $P(g_{\rm eff})$ and renormalized to plot the conditional distribution $P(g_{\rm eff}\,|\,N \neq 0)$. With $\overline{N}^0_{\rm eff} = 1$ a mean $g_{\rm eff} \approx g_{\rm max}$ is defined by the peak in the distribution. The distribution is not, however, similar to $P(g_{\rm eff}\,|\,1)$, but has an approximate Gaussian form. This form follows by the central limit theorem, indicating that $g_{\rm eff}$ is realized from a sum over many atoms [Eq. (3)]. With $\overline{N}^0_{\rm eff} = 0.02$ the simulated distribution is a good approximation to $P(g_{\rm eff}\,|\,1)$; one-atom interactions dominate. But here we encounter the real difficulty: the only peak in the one atom distribution is the singularity at $g_{\rm eff} = 0$.

Our proposal, *photon correlation spectroscopy*, resolves the difficulty. It relies on two main ideas: a scheme to excite the two-quanta entangled state resonances with a well-defined $g_{\rm eff} \neq 0$, and a method of detection which is sensitive to the decay of two-quanta states. The excitation scheme views $P(g_{\rm eff}\,|\,1)$ as a source of inhomogeneous broadening. A subpopulation of systems is then

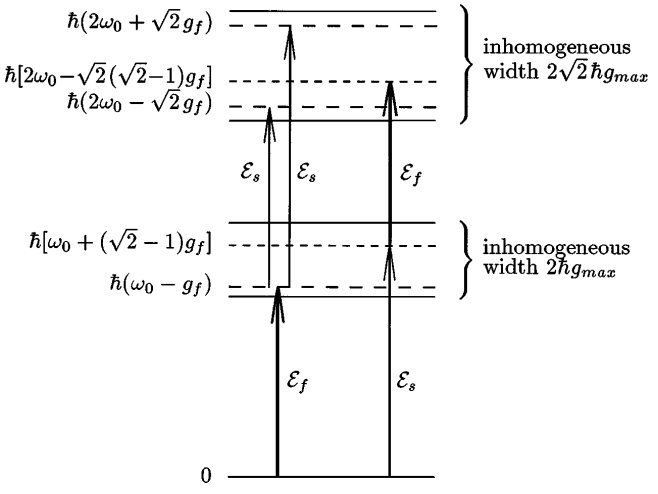


FIG. 2. Excitation of two-quanta entangled state resonances in the presence of inhomogeneous broadening.

selected using hole burning ideas. The details are illustrated in Fig. 2. Two lasers excite the atoms as they traverse the cavity, one with a fixed frequency $\omega_f$ and the other with a frequency $\omega_s$ which is scanned; the laser intensities define Rabi frequencies $\sqrt{2}\,\mathcal{E}_f$ and $\sqrt{2}\,\mathcal{E}_s$, respectively. As $\omega_s$ is scanned, three two-photon resonances occur, selectively exciting subpopulations from the $P(g_{\text{eff}})$ distribution—two resonances select $g_{\text{eff}} = g_f \equiv |\omega_f - \omega_0|$ and the other $g_{\text{eff}} = (\sqrt{2} - 1)g_f$. Thus, two-quanta entangled states are excited with well-defined $g_{\text{eff}}$. To detect these states we make an analogy with particle physics. There, unstable particle resonances are detected by correlating decay products. The signature of a two-quanta entangled state is the emission of a photon pair. Our proposal is to detect pairs of photons from the cavity and measure the rate of these coincidences as a function of $\omega_s$.

The interpretation of $P(g_{\text{eff}}\,|\,1)$ as a source of inhomogeneous broadening is essential, but certainly not always valid. Individual atoms have random speeds $v/\overline{v} = \frac{4}{3}\sqrt{\xi/\pi}$, where $\overline{v}$ is the mean speed and $\xi$ is distributed with probability density $p(\xi) = \xi e^{-\xi}$. Clearly, for sufficiently low speeds the interpretation does hold: as $g_{\text{eff}}$ changes in time, the system adiabatically follows, excited, on average, close to the steady state which would be reached with $g_{\text{eff}}$ strictly constant. With the passage of many atoms the steady-state response for fixed $g_{\text{eff}}$ is averaged against $P(g_{\text{eff}}\,|\,1)$. This picture cannot hold at arbitrarily high speeds, however. The limit is determined by the radiative lifetime (the rate to reach steady state) and the rate at which $g_{\text{eff}}$ changes due to the atomic motion. Thus, over one lifetime $g_{\text{eff}}$ should change little compared with the homogeneous width—we require $\max\{|dg_{\text{eff}}/dt|\}[\frac{1}{2}(\kappa + \gamma/2)]^{-1} < \frac{1}{2}(\kappa + \gamma/2)$, where $2\kappa$ and $\gamma$ are the radiative widths of the cavity and atom, respectively, and $\frac{1}{2}(\kappa + \gamma/2)$ is the half-width of the first excited state. This yields the condition

$$\frac{\overline{v}/w_0}{\frac{1}{2}(\kappa + \gamma/2)} < \sqrt{\frac{e}{2}}\,\frac{\frac{1}{2}(\kappa + \gamma/2)}{g_{\max}}. \tag{8}$$

Note that the speed must be significantly lower than is required when transit broadening contributes to the homogeneous width. The latter holds for $\overline{N}^0_{\text{eff}} \gg 1$, in which case Eq. (8) is replaced by $\overline{v}/w_0 < \frac{1}{2}(\kappa + \gamma/2)$. This inequality can be satisfied by a thermal atomic beam while the inequality of Eq. (8) requires slowed atoms.

Figure 3 illustrates the resonant excitation of the ground to first excited state transition by the fixed-frequency laser, selecting $g_{\text{eff}} = |\omega_f - \omega_0| = 0.5 g_{\max}$. Figures 3(a) and 3(b) plot the conditioned photon number expectation, $\langle \hat{a}^\dagger \hat{a} \rangle_c$, along one quantum trajectory [11] as four atoms traverse the cavity at regular intervals of time. For slowed atoms, strong resonant photon scattering occurs twice during the passage of each atom [Fig. 3(a)]. This $g$-selective excitation does not occur at thermal speeds [Fig. 3(b)].

To test our ideas we have carried out a numerical computation which combines a Monte Carlo simulation of the atomic beam with a quantum trajectory simulation of the photon scattering. The photons emitted through the cavity mirrors provide the data presented in Figs. 4 and 5. Figure 4 plots the number of photon counts, and Fig. 5 the number of coincidences, as a function of $\omega_s$. In (a) both lasers illuminate the atoms, in (b) only the scanned-frequency laser illuminates the atoms, and the difference between (a) and (b) is plotted in (c). The spectra before taking the difference are dominated by an inhomogeneously broadened peak centered on the

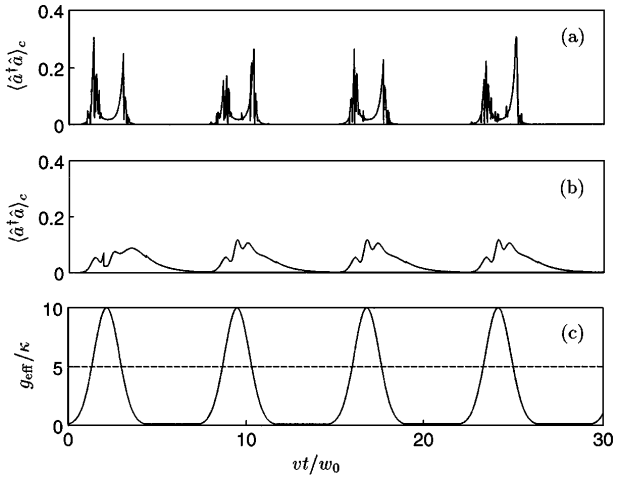


FIG. 3. Response of the conditioned photon number expectation as four atoms traverse the cavity: (a) $v = 10$m/s, (b) $v = 300$m/s, (c) time dependence of $g_{\text{eff}}$. The parameters are $w_0 = 40\ \mu$m, $\kappa/2\pi = 0.65$ MHz, $g_{\max}/\kappa = 10$, $\gamma/2\kappa = 1$, $\mathcal{E}_f/\kappa = 1$, $(\omega_f - \omega_0)/\kappa = 5$, and $\mathcal{E}_s/\kappa = 0$.

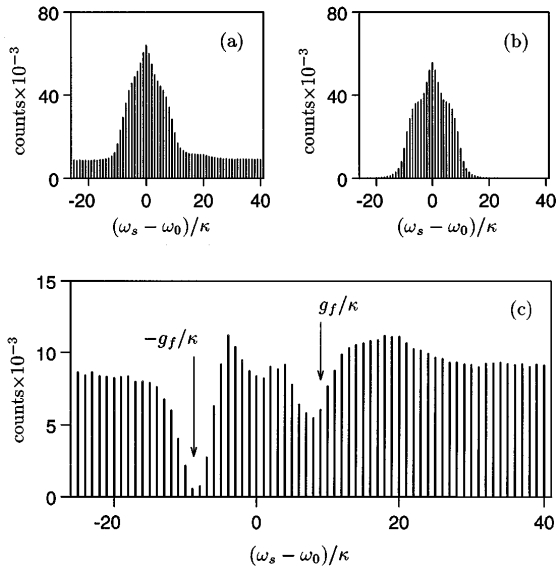


FIG. 4. Number of photon counts versus scanned frequency $\omega_s$: (a) $\mathcal{E}_f/\kappa = 0.707$, $\mathcal{E}_s/\kappa = 1.414$; (b) $\mathcal{E}_f/\kappa = 0$, $\mathcal{E}_s/\kappa = 1.414$; (c) difference spectrum (a)-(b). During the simulation $\sim 3600$ atoms traverse the cavity at an average speed $\overline{v} = 10$m/s for each setting of $\omega_s$. $(\omega_f - \omega_0)/\kappa = -9$ and the other parameters are those of Fig. 1(b) (ii) and Fig. 3.

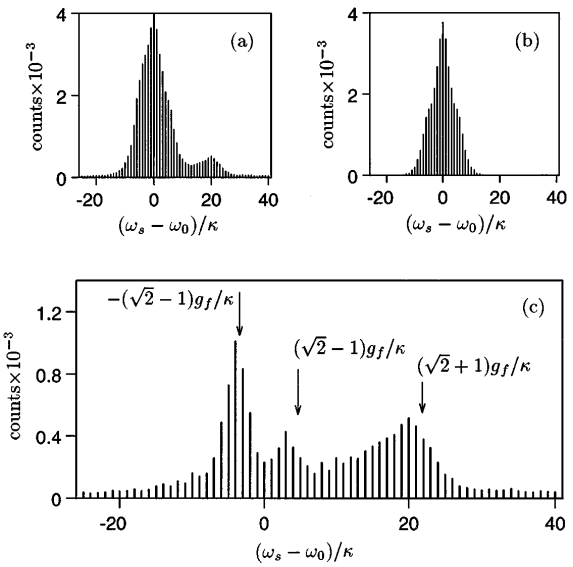


FIG. 5. Number of photon coincidence counts [separation $\tau < \tau_c \equiv 0.5(2\kappa)^{-1}$] versus scanned frequency $\omega_s$. The parameters are those of Fig. 4.

resonance frequency $\omega_0$. Nevertheless, the two-photon resonance at $\omega_s - \omega_0 = (\sqrt{2} + 1)g_f$ is already well resolved in Fig. 5(a). After the difference is taken, the photon coincidence spectrum [Fig. 5(c)] clearly shows the three two-photon resonances identified by Fig. 2. The peaks are shifted slightly, probably due to the motion of the atoms. The two-photon resonances are also apparent in Fig. 4(c), but are relatively small compared with the background. Here the prominent features are the two holes centered at frequencies $\omega_s - \omega_0 = \pm g_f$. These are Lamb dips. Thus, Lamb-dip spectroscopy can provide a direct measurement of the ground to the first excited state doublet selected by the setting of $\omega_f$.

The simulation suggests that photon correlation spectroscopy is a feasible technique for cavity QED experiments at optical frequencies. It includes the motion of the atoms (and distribution of speeds), the occasional two- or three-atom interactions which occur at nonzero atomic beam density, a realistic time window to select photon pairs, and the sampling errors which result from stochastic photon and atom counting processes. One important idealization was, however, made. In place of $V$ we used an interaction volume bounded by a mask in the $(y, z)$ plane. The mask excludes atoms that would pass far from the antinodes of the cavity mode. This strategy allowed us to increase the atomic beam density, hence the size of the subpopulations selected by hole burning, without adding more multiatom interactions. In this way, the computation time needed to achieve good statistics was reduced by an order of magnitude. We emphasize that it was numerical, not physical, considerations that suggested the use of a mask. Nevertheless, since the distribution of $g_{\text{eff}}$ is changed with its use [Fig. 6(a)], we have checked the simulation against a calculation which can be carried through both with and without a $(y, z)$-plane mask. The calculation is based on a continued fraction solution of the master equation for one atom interacting with a cavity mode in the presence of bichromatic excitation at fixed $g_{\text{eff}}$. Inhomogeneous broadening is included by taking an average against $P(g_{\text{eff}} \mid 1)$ [12]. Although the features listed above are no longer accounted for, the computation efficiency of the method is superior to the simulation by orders of magnitude.

Figure 6(b) compares the photon coincidence spectra calculated with and without the $(y, z)$-plane mask. In the absence of the mask, all three two-photon resonances remain; but with the resolution of the resonance at $(\sqrt{2} + 1)g_{\text{eff}}$ reduced. This is caused by a growth of the resonance at $(\sqrt{2} - 1)g_{\text{eff}}$, which follows from the increased weight of the subpopulation selected with $g_{\text{eff}} = (\sqrt{2} - 1)g_f$ relative to that with $g_{\text{eff}} = g_f$. Note, finally, the good agreement between the continued fraction calculation [curve (ii) of Fig. 6(b)] and the quantum trajectory simulation [Fig. 5(c)].

This work was supported by NSF under Grant No. PHY-9214501. We thank B. F. Wielinga for assistance with the continued fraction calculation.

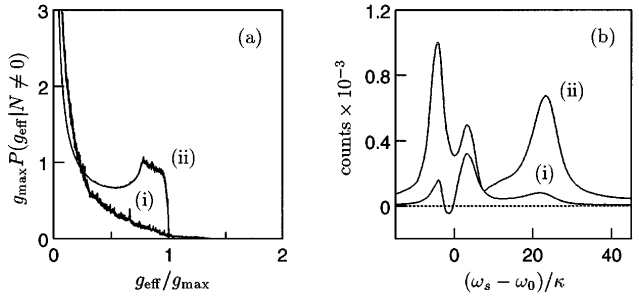


FIG. 6. (a) Distribution of $g_{\text{eff}}$: (i) without a $(y, z)$-plane mask, for $\overline{N}^0_{\text{eff}} = 0.02$, $F = 0.01$, (ii) with a $(y, z)$-plane mask $[|\cos\theta| \leq \cos(0.1\pi)$, $|y/w_0| \leq 0.5]$, for $\overline{N}^0_{\text{eff}} = 0.1$, $F = 0.01$. (b) Corresponding photon coincidence spectra calculated by the continued fraction method. The scale matches the counting times used in Figs. 4 and 5.

[1] E. T. Jaynes and F. W. Cummings, Proc. IEEE **51**, 89 (1963).
[2] M. G. Raizen *et al.*, Phys. Rev. Lett. **63**, 240 (1989).
[3] Y. Zhu *et al.*, Phys. Rev. Lett. **64**, 2499 (1990).
[4] R. J. Thompson *et al.*, Phys. Rev. Lett. **68**, 1132 (1992).
[5] F. Bernardot *et al.*, Europhys. Lett. **17**, 33 (1992).
[6] C. Weisbuch *et al.*, Phys. Rev. Lett. **69**, 3314 (1992).
[7] H. Wang *et al.*, Phys. Rev. B **51**, 14 713 (1995).
[8] S. Pau *et al.*, Phys. Rev. B **51**, 14 437 (1995).
[9] G. Rempe *et al.*, Phys. Rev. Lett. **58**, 353 (1987).
[10] M. Brune *et al.*, Phys. Rev. Lett. **76**, 1800 (1996).
[11] H. J. Carmichael, *An Open Systems Approach to Quantum Optics*, Lectures Notes in Physics Vol. M18 (Springer, Berlin, 1993).
[12] B. C. Sanders *et al.*, (unpublished).